Dynamics of two-dimensional dark quasisolitons in a smoothly inhomogeneous Bose-Einstein condensate

L. A. Smirnov* and V. A. Mironov

Institute of Applied Physics of the Russian Academy of Sciences (IAP RAS) 46 Ul'yanov Street, 603950 Nizhny Novgorod, Russia

(Received 22 March 2012; published 16 May 2012)

We develop an asymptotic theory describing the dynamics of two-dimensional dark quasisolitons in a smoothly inhomogeneous Bose-Einstein condensate (BEC) with repulsive interaction between atoms. It is shown that the trajectories of such quasisolitons coincide with the geometric-optical rays in an equivalent isotropic medium characterized by the effective refractive index dependent on both the density of the undisturbed condensate and the energy of the structures. An expression for this effective refractive index is found and specific features of the refraction of quasisolitons with different initial energies by the condensate inhomogeneities are studied. The obtained results are confirmed by direct numerical simulation using the Gross-Pitaevskii (GP) equation.

DOI: 10.1103/PhysRevA.85.053620 PACS number(s): 03.75.Lm, 03.75.Kk, 03.75.Hh, 67.85.De

I. INTRODUCTION

To understand the processes in an inhomogeneous Bose-Einstein condensate (BEC) [1–4] with repulsive interaction between atoms and to control these processes, it is of particular importance to describe the dynamics of the interacting quantum vortices [4–6]. The vortex structures arise in the condensate due to different kinds of external forcing [7,8] (using, e.g., focused laser beams [9]) or the development of modulation instabilities [10]. Numerical calculations [4,11–15] and a number of experiments [4,7,8,13,14] show that quantum vortices largely determine the long-term evolution of the BEC wave function. They are rightly associated with the breaking of the superfluidity mode [1–6,9,13–15] and the transition of the condensate to the turbulent state [5,9,16–26].

Quite recently (in 2010–2011), a few series of experiments [27–29] were conducted for controlled excitation of single vortex pairs and examination of their further dynamics in the BEC confined in disk-shaped traps, for which the model of a two-dimensional condensate is valid [1–4]. The behavior of the vortices forming a vortex pair was traced in detail in those experiments. In particular, it was noted that penetrating from a less dense into a more dense condensate, the vortex and antivortex approach each other and, on the contrary, diverge otherwise [27]. Motion with the elements of rotation of the vortex pair was observed in the vicinity of the minimum of the trap potential [28,29].

In a theoretical description of this behavior in Refs. [29–33], the interaction between vortices was calculated as in fluid mechanics using the effective dynamical equations. However, this precludes taking into account some features of the condensates of ultracold gases, and in the first place their compressibility and the fact that the cores of the quantum vortices have a finite size.

In this paper, we propose a somewhat different approach to the problem of the dynamics of vortex pairs. This approach is applicable for a smoothly inhomogeneous BEC where the distance between vortices is much smaller than the characteristic scale of inhomogeneity of the medium. In this case, the vortex pairs can be regarded as quasisoliton formations close in structure to the two-dimensional dark solitons [34–41] existing in an inhomogeneous condensate. These solitons move along a straight line at a subsonic velocity against the background of a constant-density condensate. Their energy and momentum are finite and are uniquely related to each other. The density and the velocity field disturbances of the condensate decay at large distances by a power law more rapidly than in a single vortex, similar to the field of a two-dimensional dipole in electrostatics. A fairly good spatial localization of two-dimensional dark solitons is exactly the reason why the so-called "quasisolitons," which are close to them in structure, can also be implemented in an inhomogeneous BEC.

It stands to reason to speak of quasisolitons only if their sizes are small compared with the characteristic scale of inhomogeneity of the medium. In this paper, it is shown that in an inhomogeneous BEC they are in accelerated motion and generally move not along straight lines, but along curved trajectories, which, in principle, is accompanied by the emission of density waves. However, in a smoothly inhomogeneous condensate the radiation losses are negligibly small, and the energy stored in the quasisoliton can be considered a conserved quantity, whose value strongly affects its dynamics. When moving in a smoothly inhomogeneous BEC, the two-dimensional dark quasisolitons are restructured adiabatically. As a result, the vortex pairs may convert into vortex-free solitons, which, in turn, may form vortex pairs.

In this paper, we speak of a two-dimensional problem [42], i.e., $\mathbf{r} = (x, y)$, to which, as was mentioned above, the analysis of the condensate behavior in a disk-shaped trap reduces [1–4]. The BEC with repulsive interaction between atoms can be described in the mean-field approximation using the classical wave function $\Psi(\mathbf{r},t)$, which satisfies the Gross-Pitaevskii (GP) equation [1–4]:

$$i\frac{\partial\Psi}{\partial t} + \frac{1}{2}\Delta\Psi + (1 - |\Psi|^2)\Psi = V_{\text{ext}}(\mathbf{r})\Psi. \qquad (1)$$

Here, we used the normalization [42] in which the time t, the coordinates $\mathbf{r}$, the condensate density $|\Psi(\mathbf{r},t)|^2$, and the external-force potential $V_{\text{ext}}(\mathbf{r})$ are dimensionless quantities, and the chemical potential is equal to unity.

The contents of this paper are as follows: In Sec. II, we discuss two-dimensional dark solitons and give some integral

*smirnov_lev@appl.sci-nnov.ru

relations and an approximation formula for the energy vs momentum dependence. In Sec. III, we derive a self-consistent system of equations which relate the integral characteristics of a soliton and the trajectory of its propagation in a smoothly inhomogeneous BEC. In Sec. IV, this system is reduced to the usual geometric-optical form with the only difference that the effective refractive index is determined not only by the properties of the undisturbed condensate, but also by the energy of the soliton formation. In Sec. V, by comparing with the results of numerical calculations performed directly within the framework of the GP equation, it is demonstrated that the theory we developed adequately describes the dynamics of two-dimensional dark solitons in a smoothly inhomogeneous BEC. In the Conclusions section (Sec. VI), we sum up the work done.

II. TWO-DIMENSIONAL DARK SOLITONS IN A HOMOGENEOUS BEC

The GP equation (1) with $V_{\text{ext}}(\mathbf{r}) = 0$ has a single-parameter family of solutions in the form of two-dimensional dark solitons moving (for definiteness, along the x axis) at a constant velocity $\bar{v}$. They are described by a wave function of the form $\Psi_s(\xi = (x - \bar{v}t), y, \bar{v})$, which satisfies the stationary equation

$$-i\bar{v}\frac{\partial \Psi_s}{\partial \xi} + \frac{1}{2}\frac{\partial^2 \Psi_s}{\partial \xi^2} + \frac{1}{2}\frac{\partial^2 \Psi_s}{\partial y^2} + (1 - |\Psi_s|^2)\Psi_s = 0 \tag{2}$$

and the boundary conditions at infinity,

$$\Psi_s(\sqrt{\xi^2 + y^2} \to \infty) \to 1. \tag{3}$$

Here, $\bar{v}$ plays the role of the problem parameter. Depending on $\bar{v}$, two-dimensional dark solitons can be "vortex" and "vortex free." In the first case, they are the so-called vortex pairs (or dipoles), in which the BEC density at two points (the so-called "topological defects") located on the line perpendicular to the direction of motion becomes zero. The Bose gas in the vicinity of these points "rotates" in opposite directions. Vortex-free solitons are characterized by the absence of zeros of the density. In the weakly nonlinear limit, where the value of $|\bar{v}|$ tends to the sound velocity ($|\bar{v}| \to 1$), they coincide with known solutions of the Kadomtsev-Petviashvili (KP) equation [43–46].

The properties of the two-dimensional dark solitons were studied in detail in Refs. [34–40]. It was shown there that the vortex pairs are implemented for $0 < |\bar{v}| < 0.61$ and the vortex-free solitons, for $0.61 < |\bar{v}| < 1$. When $|\bar{v}| = \bar{v}_* \approx 0.61$, there is a continuous transition from the vortex state with two zeros of the density into a vortex-free state, in which the density is different from zero everywhere. We are dealing with a specific bifurcation, in which the two-dimensional dark soliton "casts off" the circulation [34–37].

Two-dimensional dark solitons can be regarded as solutions of the variation problem

$$\delta(\mathcal{H} - \bar{v}\mathcal{P}_x) = 0, \tag{4}$$

where

$$\mathcal{H} = \frac{1}{2}\int_{-\infty}^{+\infty} dy \int_{-\infty}^{+\infty} d\xi [|\nabla\Psi|^2 + (1 - |\Psi|^2)^2], \tag{5}$$

$$\mathbf{P} = \frac{i}{2}\int_{-\infty}^{+\infty} dy \int_{-\infty}^{+\infty} d\xi (\Psi\nabla\Psi^* - \Psi^*\nabla\Psi) \tag{6}$$

are the Hamiltonian and the momentum of the Bose condensate, respectively. From this variation formulation, it is easy to find the following integral relations for two-dimensional dark solitons [36,47]:

$$\bar{\mathcal{E}} \equiv \mathcal{H}_s = \int_{-\infty}^{+\infty} dy \int_{-\infty}^{+\infty} d\xi \left|\frac{\partial \Psi_s}{\partial \xi}\right|^2, \tag{7}$$

$$\bar{\mathcal{E}} - \bar{v}\bar{\mathcal{P}} = \int_{-\infty}^{+\infty} dy \int_{-\infty}^{+\infty} d\xi \left|\frac{\partial \Psi_s}{\partial y}\right|^2, \tag{8}$$

$$\bar{v}\bar{\mathcal{P}} = \int_{-\infty}^{+\infty} dy \int_{-\infty}^{+\infty} d\xi (1 - |\Psi_s|^2)^2, \tag{9}$$

where $\bar{\mathcal{E}}$ is the energy of a soliton and $\bar{\mathcal{P}} \equiv \mathcal{P}_{s_x}$ is the projection of its momentum on the x axis (by virtue of the symmetry of the problem, $\mathcal{P}_{s_y} = 0$). The velocity $\bar{v}$ of a two-dimensional dark soliton $\Psi_s(\xi, y, \bar{v})$ is defined as

$$\bar{v} = \frac{d\bar{\mathcal{E}}}{d\bar{\mathcal{P}}} < \frac{\bar{\mathcal{E}}}{\bar{\mathcal{P}}}. \tag{10}$$

This inequality is a direct consequence of Eqs. (7)–(9). According to this inequality, the curve $\bar{\mathcal{E}} = \bar{\mathcal{E}}(\bar{\mathcal{P}})$ is located below the straight line $\bar{\mathcal{E}} = \bar{\mathcal{P}}$.

At $\sqrt{\xi^2 + y^2} \to \infty$, the wave function of a two-dimensional dark soliton can be represented as

$$\Psi_s(\xi, y, \bar{v}) = \left(1 + \tfrac{1}{2}\tilde{n}_s(\xi, y, \bar{v})\right)\exp[i\tilde{\theta}_s(\xi, y, \bar{v})], \tag{11}$$

where $\tilde{n}_s(\xi, y, \bar{v})$ and $\tilde{\theta}_s(\xi, y, \bar{v})$ are the perturbations of the BEC density and phase, which behave as follows:

$$\tilde{n}_s(\sqrt{\xi^2 + y^2} \to \infty) \approx -\bar{v}\frac{\partial}{\partial \xi}\left(\frac{\bar{\varpi}\xi}{[\xi^2 + (1 - \bar{v}^2)y^2]}\right), \tag{12}$$

$$\tilde{\theta}_s(\sqrt{\xi^2 + y^2} \to \infty) \approx \frac{\bar{\varpi}\xi}{[\xi^2 + (1 - \bar{v}^2)y^2]}. \tag{13}$$

Here, $\bar{\varpi}$ is the real value (analog of the dipole moment of the charge or current distribution in electrodynamics).

Multiplying (2) by $\Psi_s^*(\xi, y, \bar{v})$, integrating the real part over ξ and y in infinite limits, and making use of the asymptotic behavior of the wave function of a two-dimensional dark soliton for $\sqrt{\xi^2 + y^2} \to \infty$, we arrive at another useful equality, which makes it possible to determine the energy $\bar{\mathcal{E}}$ without calculating the derivatives of the wave function $\Psi(\xi, y)$, but directly from the density distribution $n_s(\xi, y, \bar{v}) = |\Psi_s(\xi, y, \bar{v})|^2$:

$$\bar{\mathcal{E}} = \bar{\mathcal{N}} + \bar{v}\bar{\mathcal{P}}/2, \tag{14}$$

where

$$\bar{\mathcal{N}} = \int_{-\infty}^{+\infty} dy \int_{-\infty}^{+\infty} d\xi (1 - |\Psi_s|^2), \tag{15}$$

and $\bar{v}\bar{P}$ is found from integral relation (9).

Two-dimensional dark soliton solutions with $\bar{\mathcal{E}} \gg 1$ ($\bar{v} \ll 1$) are vortex pairs, whose wave function is well described by the expression

$$\Psi_s(\xi, y, \bar{v}) \approx \psi_{\rm VP}(\xi, y, \bar{v}) \exp(i\theta_{\rm VP}(\xi, y, \bar{v})), \tag{16}$$

where $\theta_{\rm VP}(\xi, y, \bar{v}) = \varphi_1(\xi, y, \bar{v}) - \varphi_2(\xi, y, \bar{v})$ is the phase of the vortex pair, $\varphi_1(\xi, y, \bar{v})$ and $\varphi_2(\xi, y, \bar{v})$ are the polar angles around the points $(\xi = 0, y = l/2)$ and $(\xi = 0, y = -l/2)$, respectively, and $l = l(\bar{v})$ is the distance between topological defects (zeroes of the density) [48–52]. Near the points $(\xi = 0, y = \pm l/2)$, the density $n_{\rm VP} = \psi_{\rm VP}^2$ and the phase $\theta_{\rm VP}$ of the Bose condensate behave as in single vortices, namely, $n_{\rm VP}(r_{1,2} \to 0) \propto r_{1,2}^2$ and $\theta_{\rm VP}(r_{1,2} \to 0) \approx \varphi_{1,2}$, where $r_{1,2}^2 = \xi^2 + (y \mp l/2)^2$.

When $\bar{\mathcal{E}} \gg 1$, the energy $\bar{\mathcal{E}}$, momentum $\bar{\mathcal{P}}$, and velocity $\bar{v}$ in the vortex pairs are related with l by the equations [48–53]

$$\bar{\mathcal{E}} \approx 2\pi \ln(l), \quad \bar{\mathcal{P}} \approx 2\pi l, \quad \bar{v} \approx 1/l. \tag{17}$$

It is seen from Eq. (17) that for $\bar{\mathcal{E}} \gg 1$ the dependencies $\bar{\mathcal{P}}(\bar{\mathcal{E}})$ and $\bar{v}(\bar{\mathcal{E}})$ have the following form:

$$\bar{\mathcal{P}}(\bar{\mathcal{E}} \gg 1) \approx 2\pi \exp(\bar{\mathcal{E}}/2\pi.), \tag{18}$$

$$\bar{v}(\bar{\mathcal{E}} \gg 1) \approx \exp(-\bar{\mathcal{E}}/2\pi.). \tag{19}$$

In the weakly nonlinear limit, where the soliton velocity tends to the sound velocity ($\bar{v} \to 1$), and the soliton energy is small, i.e., ($\bar{\mathcal{E}} \ll 1$), the solitary waves in the BEC can be sought in the form of an asymptotic expansion in a small parameter ϵ [36,41,54]:

$$n(t, \mathbf{r}) = 1 + \sum_{j=1}^{\infty} \epsilon^j n_j(T, X, Y), \tag{20}$$

$$\theta(t, \mathbf{r}) = \sum_{j=1}^{\infty} \epsilon^{(j-1/2)} \theta_j(T, X, Y), \tag{21}$$

where $n(t, \mathbf{r}) = |\Psi(t, \mathbf{r})|^2$ is the density of the condensate and $\theta(t, \mathbf{r})$ is the phase of its wave function. In Eqs. (20) and (21), we introduced "slow" time and coordinates

$$T = \epsilon^{3/2} t, \quad X = \epsilon^{1/2}(x - t), \quad Y = \epsilon y. \tag{22}$$

In the case of a homogeneous condensate [$V_{\rm ext}(\mathbf{r}) = 0$], taking into account Eqs. (20)–(22) from GP equation (1), we obtain for $n_1(T, X, Y)$ and $\theta_1(T, X, Y)$ the KP equation [36,41,54]

$$\frac{\partial \theta_1}{\partial T} + \frac{3}{2} \frac{\partial (n_1 \theta_1)}{\partial X} - \frac{1}{8} \frac{\partial^3 \theta_1}{\partial X^3} = \frac{1}{2} \frac{\partial^2 n_1}{\partial Y^2}, \quad n_1 = -\frac{\partial \theta_1}{\partial X}. \tag{23}$$

Using the replacement

$$n_1 = \frac{\partial^2}{\partial X^2} [\ln \Phi((X + \epsilon^{-1} \tilde{v}_{\rm KP} T), Y)], \tag{24}$$

it can be shown [43–46] that KP equation (23) has soliton solutions localized both in the X and Y coordinates. For these solutions, the parameter ϵ has the same order of smallness as the positive-definite quantity $\tilde{v}_{\rm KP} = (1 - \bar{v})$, which describes the deviation of the two-dimensional dark soliton velocity $\bar{v}$ from the sound velocity. In variables ξ and y, the main terms of expansion given by Eqs. (20) and (21) are, respectively,

$$n_{s,1}(\xi, y, \bar{v}) = \epsilon n_1 = \frac{16 \tilde{v}_{\rm KP} \left[3 - 8 \tilde{v}_{\rm KP} \xi^2 + 16 \tilde{v}_{\rm KP}^2 y^2\right]}{\left[3 + 8 \tilde{v}_{\rm KP} \xi^2 + 16 \tilde{v}_{\rm KP}^2 y^2\right]^2}, \tag{25}$$

$$\theta_{s,1}(\xi, y, \bar{v}) = \epsilon^{1/2} \theta_1 = \frac{16 \tilde{v}_{\rm KP} \xi}{\left[3 + 8 \tilde{v}_{\rm KP} \xi^2 + 16 \tilde{v}_{\rm KP}^2 y^2\right]}. \tag{26}$$

Here, the subscript "s" stands for the solitons.

Substituting Eqs. (20) and (21) with allowance for Eqs. (25) and (26) into Eq. (7), upon integration over ξ and y we find the relation between $\tilde{v}_{\rm KP}$ and $\bar{\mathcal{E}}$:

$$\tilde{v}_{\rm KP} = [1 - \bar{v}(\bar{\mathcal{E}} \ll 1)] \approx \frac{9}{128\pi^2} \bar{\mathcal{E}}^2. \tag{27}$$

Hence, using Eq. (10), we find that in the low-energy limit ($\bar{\mathcal{E}} \ll 1$) the momentum $\bar{\mathcal{P}}$ of two-dimensional dark solitons is related with $\bar{\mathcal{E}}$ by the equation

$$\bar{\mathcal{P}}(\bar{\mathcal{E}} \ll 1) \approx \bar{\mathcal{E}} - \frac{3}{128\pi^2} \bar{\mathcal{E}}^3. \tag{28}$$

We picked up a fairly simple analytical approximation for the dependence $\bar{\mathcal{P}}(\bar{\mathcal{E}})$, which everywhere (for any value of $\bar{\mathcal{E}}$) agrees very well with the results obtained by numerical solution of stationary equation (2):

$$\bar{\mathcal{P}}(\bar{\mathcal{E}}) = \alpha(\bar{\mathcal{E}}) \sinh[\bar{\mathcal{E}}/\alpha(\bar{\mathcal{E}}).], \tag{29}$$

where

$$\alpha(\bar{\mathcal{E}}) = 2\pi + (2\pi/3.) \exp\left(-\bar{\mathcal{E}}^2/\sigma_{\bar{\mathcal{E}}}^2\right). \tag{30}$$

When $\bar{\mathcal{E}} \gg 1$, function (29) tends to (18), and for $\bar{\mathcal{E}} \ll 1$ it converts into (28). If the constant $\sigma_{\bar{\mathcal{E}}}$ is chosen equal to

$$\sigma_{\bar{\mathcal{E}}} = 9.8, \tag{31}$$

then the difference of Eq. (29) from the results of the numerical solution of Eq. (2) with boundary conditions (3) is minimal (the relative error does not exceed 1%). This is clearly demonstrated in Fig. 1, in which the unshared squares and circles show the results of numerical calculations and the solid lines represent the dependencies $\bar{\mathcal{P}}(\bar{\mathcal{E}})$ and $\bar{v}(\bar{\mathcal{E}})$ obtained using approximation (29)–(31).

III. ASYMPTOTIC DESCRIPTION OF THE DYNAMICS OF TWO-DIMENSIONAL DARK QUASISOLITONS IN A SMOOTHLY INHOMOGENEOUS BEC

We represent the wave function $\Psi(\mathbf{r}, t)$ of the BEC as the product

$$\Psi(\mathbf{r}, t) = G(\mathbf{r}) F(\mathbf{r}, t) \tag{32}$$

by extracting as a cofactor its "undisturbed" part $G(\mathbf{r})$, which is formed under the action of the external potential $V_{\rm ext}(\mathbf{r})$ and satisfies the stationary GP equation

$$\tfrac{1}{2} \Delta G + (1 - |G|^2) G - V_{\rm ext}(\mathbf{r}) G = 0. \tag{33}$$

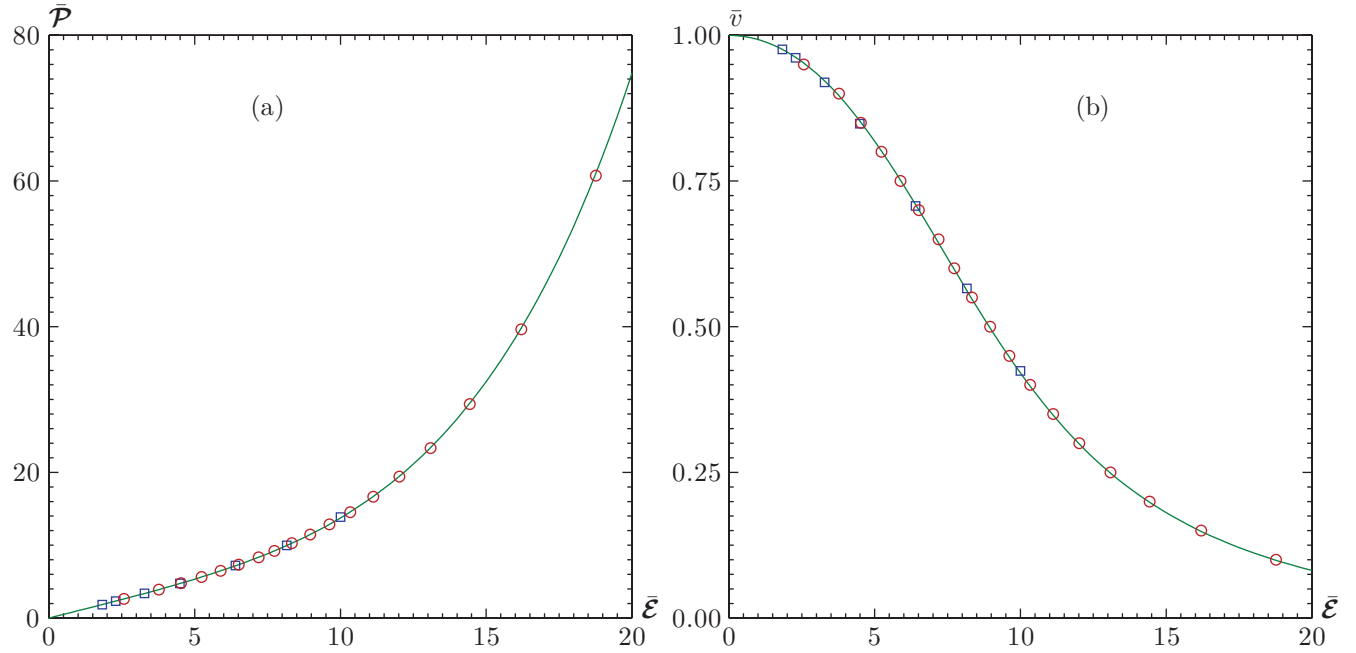

FIG. 1. (Color online) Dependencies (a) of the momentum $\bar{\mathcal{P}}$ and (b) of the velocity $\bar{v}$ of a two-dimensional dark soliton on its energy $\bar{\mathcal{E}}$. The results obtained by the authors of this paper by numerical solution of stationary equation (2) are marked by unshaded circles. Unshaded squares correspond to the data taken from [34,35]. Solid lines show the diagrams of the functions $\bar{\mathcal{P}}(\bar{\mathcal{E}})$ and $\bar{v}(\bar{\mathcal{E}})$ corresponding to approximation (29)–(31).

Then for the function $F(\mathbf{r},t)$ describing the behavior of the finite-amplitude disturbances in an initially inhomogeneous BEC, it is easy to obtain the following nonlinear dynamic equation:

$$i\frac{\partial F}{\partial t}+\frac{1}{2}\Delta F+|G|^2(1-|F|^2)F=-\frac{1}{G}\nabla G\cdot\nabla F. \quad (34)$$

Here $\nabla G\cdot\nabla F$ is the scalar product of complex vectors.

Assume that the function $G(\mathbf{r})$ and, therefore, the potential $V_{\text{ext}}(\mathbf{r})$ are gradually varied within the limits of a characteristic size Λ_{qs} of the localization region of the considered disturbance initially specified in the form of a two-dimensional quasisoliton structure. In other words, there is a small parameter in the problem, namely,

$$\mu=\Lambda_{\text{qs}}/\Lambda_G\ll 1, \quad (35)$$

where $\Lambda_G\sim|G|/|\nabla G|$ is a characteristic scale of the wave function $G(\mathbf{r})$ of the undisturbed condensate.

In the further analysis, we focus on the dynamics of a quasisoliton in the condensate at rest, such that

$$G(\mathbf{r})=g(\mathbf{r})\exp(i\theta_g), \quad (36)$$

where $g(\mathbf{r})$ is the real function of the coordinates $\mathbf{r}$ and $\theta_g=$ const is the real constant phase of the BEC [55].

For two-dimensional dark quasisolitons, Λ_{qs} is always greater than or of the order of the "local correlation radius" r_c, which in the dimensionless variables used is related with $|G(\mathbf{r})|$ by the equation

$$r_c=1/|G|\lesssim\Lambda_{\text{qs}}. \quad (37)$$

From inequalities (35) and (37) it follows that $\Lambda_G\gg r_c$. Hence, the BEC density $n_g(\mathbf{r})=g^2(\mathbf{r})$ in the stationary state can be calculated in the Thomas-Fermi approximation [1–4] by the formula

$$n_{g_{\text{TF}}}(\mathbf{r})=g^2_{\text{TF}}(\mathbf{r})=[1-V_{\text{ext}}(\mathbf{r})]>0, \quad (38)$$

neglecting the term $\Delta G/2$ (the so-called "quantum-mechanical pressure") in Eq. (33). It is easy to see that in the limit $n_{g_{\text{TF}}}(\mathbf{r})\to 0$ inequalities (35) and (37) are violated, and the proposed theory is no longer effective.

Assume that the trajectory (see Fig. 2), along which a two-dimensional dark quasisoliton propagates, is known and is defined as a function of the arc length s, namely, $\mathbf{r}_0=\mathbf{r}_0(s)$. Then the radius vector $\mathbf{r}=x\mathbf{x}_0+y\mathbf{y}_0$ [$\mathbf{x}_0$ and $\mathbf{y}_0$ are the unit vectors of the Cartesian coordinate system (x,y)] of any point M located near the trajectory $\mathbf{r}_0(s)$ can be represented as

$$\mathbf{r}=\mathbf{r}_0(s)+\eta\mathbf{n}_0(s), \quad (39)$$

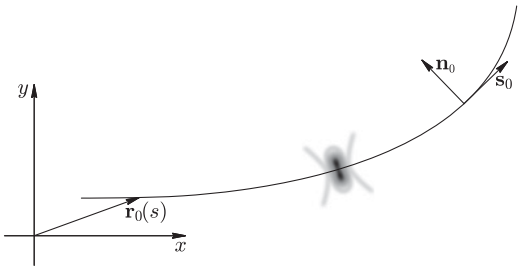

FIG. 2. A schematic representation of propagation of a two-dimensional dark quasisoliton moving along the trajectory $\mathbf{r}_0(s)$ in a smoothly inhomogeneous BEC. Here, $\mathbf{s}_0$ and $\mathbf{n}_0$ are the unit vectors of the tangent and the normal to the curve $\mathbf{r}_0(s)$.

where η is the distance along the normal dropped from the point M on the curve $\mathbf{r}_0(s)$ and $\mathbf{n}_0(s)$ is a unit vector of the normal to $\mathbf{r}_0(s)$. Equation (39) relates the Cartesian coordinates (x,y) with the orthogonal curvilinear coordinates (s,η), the transition to which is characterized by the following Lamé coefficients:

$$h_s = (1-\kappa\eta), \quad h_\eta = 1, \tag{40}$$

where $\kappa = \kappa(s)$ is the curvature of the line $\mathbf{r}_0(s)$.

Rewrite Eq. (34) in terms of the variables s and η:

$$i\frac{\partial F}{\partial t} + \frac{1}{2h_s h_\eta}\left[\frac{\partial}{\partial s}\left(\frac{h_\eta}{h_s}\frac{\partial F}{\partial s}\right) + \frac{\partial}{\partial \eta}\left(\frac{h_s}{h_\eta}\frac{\partial F}{\partial \eta}\right)\right] + |G|^2(1-|F|^2)F = -\frac{1}{G}\left[\frac{1}{h_s^2}\frac{\partial G}{\partial s}\frac{\partial F}{\partial s} + \frac{1}{h_\eta^2}\frac{\partial G}{\partial \eta}\frac{\partial F}{\partial \eta}\right]. \tag{41}$$

We will use the assumption that the characteristic variation scale Λ_G of the function $G(\mathbf{r})$ significantly exceeds the sizes Λ_{qs} of the localization region of the quasisoliton. For smooth propagation paths, the curvature $\kappa(s)$ of the trajectory of a two-dimensional dark quasisoliton can be assumed of the order of Λ_G^{-1} ($\kappa \sim \Lambda_G^{-1}$). Expanding the function $|G(\mathbf{r})|^2$ near the curve $\mathbf{r}_0(s)$ into a Taylor series of η, namely,

$$|G(\mathbf{r})|^2 = |G(\mathbf{r}_0+\eta\mathbf{n}_0)|^2 \approx |G(\mathbf{r}_0)|^2 + \left[\frac{\partial |G|^2}{\partial \eta}\right]\Big|_{\eta=0}\eta + \cdots,$$

we arrive at the following equation for $F(\mathbf{r},t)$:

$$i\frac{\partial F}{\partial t} + \frac{1}{2}\frac{\partial^2 F}{\partial s^2} + \frac{1}{2}\frac{\partial^2 F}{\partial \eta^2} + |G(\mathbf{r}_0)|^2(1-|F|^2) = -\kappa\eta\frac{\partial^2 F}{\partial s^2} + \frac{1}{2}\kappa\frac{\partial F}{\partial \eta} - \left[\frac{\partial |G|^2}{\partial \eta}\right]\Big|_{\eta=0}\eta(1-|F|^2)F - \left[\frac{1}{G}\frac{\partial G}{\partial s}\right]\Big|_{\eta=0}\frac{\partial F}{\partial s} - \left[\frac{1}{G}\frac{\partial G}{\partial \eta}\right]\Big|_{\eta=0}\frac{\partial F}{\partial \eta} + o(\mu^2). \tag{42}$$

Here $o(\mu^2)$ are terms of the order of smallness μ^2 or higher.

For the localized two-dimensional quasisoliton formation moving along the trajectory $\mathbf{r}_0(s)$ in Eq. (42), it is convenient to pass from the length s to the coordinate "accompanying" the quasisoliton:

$$\xi = s - s_{qs}(t), \quad s_{qs}(t) = \int_0^t v(t)\,dt, \tag{43}$$

where $s_{qs}(t)$ is the position of the center of a quasisoliton on the curve $\mathbf{r}_0(s)$, and $v(t)$ is its velocity. After such a transition, the solution of Eq. (42) near the curve $\mathbf{r}_0(s)$ can be represented as an asymptotic series of μ:

$$F(\xi,\eta,t) = \mu^0 F_0(\xi,\eta,v(\mu t)) + \mu^1 F_1(\xi,\eta,\mu t) + \mu^2 F_2(\xi,\eta,\mu t) + \cdots. \tag{44}$$

In the zeroth order of smallness in μ, for F_0 we obtain the "stationary" equation

$$-iv\frac{\partial F_0}{\partial \xi} + \frac{1}{2}\frac{\partial^2 F_0}{\partial \xi^2} + \frac{1}{2}\frac{\partial^2 F_0}{\partial \eta^2} + g^2(s_{qs},0)(1-|F_0|^2)F_0 = 0. \tag{45}$$

Here $g^2(s_{qs},0)$ is the density of the undisturbed inhomogeneous condensate at the center of the quasisoliton. If the coordinates, time, and velocity are normalized as

$$\bar{\mathbf{r}} = g(s_{qs},0)\mathbf{r}, \quad d\bar{t} = g^2(s_{qs},0)dt, \tag{46}$$

$$\bar{v} = v/g(s_{qs},0), \tag{47}$$

then Eq. (45) converts into Eq. (2) and has therefore a solution in the form of two-dimensional dark solitons:

$$F_0(\xi,\eta,v) \equiv \Psi_s(\bar{\xi},\bar{\eta},\bar{v}). \tag{48}$$

In the first order of smallness in μ, for the function F_1 we obtain the linear inhomogeneous differential equation in terms of the new variables $\bar{\xi}$, $\bar{\eta}$, and $\bar{t}$:

$$-i\bar{v}\frac{\partial F_1}{\partial \bar{\xi}} + \frac{1}{2}\frac{\partial^2 F_1}{\partial \bar{\xi}^2} + \frac{1}{2}\frac{\partial^2 F_1}{\partial \bar{\eta}^2} + (1-2|F_0|^2)F_1 - F_0^2 F_1^* = \mathcal{R}(F_0,\bar{v},\bar{\kappa}), \tag{49}$$

where

$$\mathcal{R}(F_0,\bar{v},\bar{\kappa}) = -\bar{\kappa}\bar{\eta}\frac{\partial^2 F_0}{\partial \bar{\xi}^2} + \frac{1}{2}\bar{\kappa}\frac{\partial F_0}{\partial \bar{\eta}} - \mathcal{A}_s\frac{\partial F_0}{\partial \bar{\xi}} - \mathcal{A}_\eta\frac{\partial F_0}{\partial \bar{\eta}} - 2\mathcal{A}_s\bar{\xi}(1-|F_0|^2)F_0 - 2\mathcal{A}_\eta\bar{\eta}(1-|F_0|^2)F_0 - i\bar{v}\mathcal{A}_s\bar{\xi}\frac{\partial F_0}{\partial \bar{\xi}} - i\bar{v}\mathcal{A}_s\bar{\eta}\frac{\partial F_0}{\partial \bar{\eta}} - i\frac{d\bar{v}}{d\bar{t}}\frac{\partial F_0}{\partial \bar{v}}, \tag{50}$$

$$\bar{\kappa}(s_{qs}) = \kappa(s_{qs})/g(s_{qs},0), \tag{51}$$

$$\mathcal{A}_s = \left[\frac{1}{g^2}\frac{\partial g}{\partial s}\right]\Big|_{\substack{s=s_{qs}\\ \eta=0}}, \quad \mathcal{A}_\eta = \left[\frac{1}{g^2}\frac{\partial g}{\partial \eta}\right]\Big|_{\substack{s=s_{qs}\\ \eta=0}}. \tag{52}$$

Differentiating Eq. (45) with respect to $\bar{\xi}$ and $\bar{\eta}$, it can easily be verified that the derivatives $\partial_{\bar{\xi}}F_0$ and $\partial_{\bar{\eta}}F_0$ are the solutions of homogeneous (with the zero right-hand side) equation (49). Multiplying Eq. (49) by $\partial_{\bar{\xi}}F_0^*$ ($\partial_{\bar{\eta}}F_0^*$), we sum up the result with the complex conjugate equation and integrate over $\bar{\xi}$ and $\bar{\eta}$ in the infinite limits. As a result, we find that the conditions for the existence of localized (both in $\bar{\xi}$ and $\bar{\eta}$) solutions in Eq. (49) are the fulfillment of the following equalities [10,56]:

$$\mathrm{Re}\left[\int_{-\infty}^{+\infty}d\bar{\eta}\int_{-\infty}^{+\infty}d\bar{\xi}\,\mathcal{R}(F_0,\bar{v},\bar{\kappa})\frac{\partial F_0^*}{\partial \bar{\xi}}\right] = 0, \tag{53}$$

$$\mathrm{Re}\left[\int_{-\infty}^{+\infty}d\bar{\eta}\int_{-\infty}^{+\infty}d\bar{\xi}\,\mathcal{R}(F_0,\bar{v},\bar{\kappa})\frac{\partial F_0^*}{\partial \bar{\eta}}\right] = 0. \tag{54}$$

These relations for the complex equation (49) are essentially counterparts of the Fredholm theorem on alternative [57].

Using the symmetry of considered localized structures, namely, $\Psi_s(\bar{\xi},\bar{\eta},\bar{v}) = \Psi_s(\bar{\xi},-\bar{\eta},\bar{v})$, and the integral relations (7)–(9), Eqs. (53) and (54) can be transformed to

$$\frac{d\bar{\mathcal{P}}}{d\bar{t}} = -2\mathcal{A}_s\bar{\mathcal{E}}, \tag{55}$$

$$\bar{\kappa} = \mathcal{A}_\eta(1 - 2\bar{\mathcal{E}}/\bar{v}\bar{\mathcal{P}}). \tag{56}$$

Here, $\bar{\kappa} = \bar{\kappa}[s_{qs}(t)]$ is the function of position of the quasisoliton $s_{qs}(t)$ on the curve $\mathbf{r}_0(s)$, which is related with the curvature $\kappa[s_{qs}(t)]$ by Eq. (51), and $\bar{v}(t)$ is the normalized quasisoliton velocity which we defined earlier in Eq. (47) as $\bar{v}(t) = v(t)/g(s_{qs}(t),0)$. The quantities $\bar{\mathcal{P}} = \bar{\mathcal{P}}(\bar{v}(t))$ and $\bar{\mathcal{E}} = \bar{\mathcal{E}}(\bar{v}(t))$ at each moment of time t are the corresponding characteristics [see Eqs. (7)–(9)] of a two-dimensional dark soliton propagating with the velocity $\bar{v}(t)$ for a given value of $\bar{v}$ in a homogeneous condensate of unit density. Hereafter we call $\bar{\mathcal{P}}(\bar{v}(t))$ and $\bar{\mathcal{E}}(\bar{v}(t))$ the normalized momentum and the normalized energy of a quasisoliton, respectively.

IV. GEOMETRIC OPTICS OF TWO-DIMENSIONAL DARK QUASISOLITONS IN A SMOOTHLY INHOMOGENEOUS BEC

Rewrite equality (55) in the form

$$\frac{1}{\bar{\mathcal{E}}}\frac{d\bar{\mathcal{E}}}{d\bar{\mathcal{P}}}\frac{d\bar{\mathcal{P}}}{d\bar{s}_{qs}} = -2\left[\frac{\partial \ln g}{\partial \bar{s}}\right]\Bigg|_{\substack{\bar{s}=\bar{s}_{qs}\\ \bar{\eta}=0}}. \tag{57}$$

Here, we took into account that

$$\frac{d\bar{s}_{qs}}{d\bar{t}} = \bar{v} = \frac{d\bar{\mathcal{E}}}{d\bar{\mathcal{P}}}. \tag{58}$$

From Eq. (57) we obtain the following integral of motion:

$$\mathcal{E}(s_{qs}) = g^2(s_{qs},0)\bar{\mathcal{E}}(s_{qs}) = g^2(0,0)\bar{\mathcal{E}}(0), \tag{59}$$

where $(s_{qs},0)$ is the position of the center of the two-dimensional dark quasisoliton, which is determined in the coordinate system (s,η), $\bar{\mathcal{E}}(0)$ are the initial values (for $t=0$) of the normalized energy of the quasisoliton, and $g^2(0,0)$ is the density of the undisturbed inhomogeneous condensate at the point $(s_{qs}(t=0) = 0,0)$, from which the quasisoliton starts.

Relation (59) can be treated as the energy conservation law for a two-dimensional dark quasisoliton moving along the trajectory $\mathbf{r}_0(s)$ in a smoothly inhomogeneous BEC. Indeed, within the localization region of the structure considered, i.e., where $\sqrt{\xi^2+\eta^2} < \Lambda_{qs}$, the wave function of the condensate $\Psi(\mathbf{r},t) = G(\mathbf{r})F(\mathbf{r},t)$ with allowance only for terms of the zeroth order of smallness in μ is the wave function of a two-dimensional dark soliton in a homogeneous BEC with density equal to $g^2(s_{qs},0)$:

$$\Psi(\mathbf{r},t) \approx G(s_{qs},0)F_0(\xi,\eta,v). \tag{60}$$

The energy $\mathcal{E}(v)$ of such solitons is a factor of $g^2(s_{qs},0)$ different from the energy $\bar{\mathcal{E}}(\bar{v})$ of the solitons in a homogeneous condensate of unit density:

$$\mathcal{E} = g^2(s_{qs},0)\bar{\mathcal{E}}. \tag{61}$$

As was mentioned above, the normalized momentum $\bar{\mathcal{P}}$ and the normalized velocity $\bar{v}$ are single-valued functions of the normalized energy $\bar{\mathcal{E}}$; hence, according to Eq. (59), both $\bar{\mathcal{P}}$ and $\bar{v}$ are functions of only $g(s_{qs},0)$, i.e., $\bar{\mathcal{P}} = \bar{\mathcal{P}}(g(s_{qs},0))$ and $\bar{v} = \bar{v}(g(s_{qs},0))$. It follows immediately that an increase (decrease) in the density $n_g(s_{qs},0) = g^2(s_{qs},0)$ of the undisturbed condensate along the propagation path leads to a consistent decrease (increase) in $\bar{\mathcal{E}}(s_{qs})$ and $\bar{\mathcal{P}}(s_{qs})$ and an increase (decrease) in $\bar{v}(s_{qs})$. As a result, the vortex pair as it penetrates into the more dense condensate may become a vortex-free soliton, and vice versa the vortex-free soliton as it reaches the less dense Bose gas may convert into a vortex pair.

Rewriting Eq. (56) for the non-normalized curvature $\kappa(\bar{s}_{qs}) = g(s_{qs},0)\bar{\kappa}(s_{qs})$, we have

$$\kappa(s_{qs}) = \left(1 - \frac{2\bar{\mathcal{E}}(g(s_{qs},0))}{\bar{v}(g(s_{qs},0))\bar{\mathcal{P}}(g(s_{qs},0))}\right)\left[\frac{\partial \ln g}{\partial \eta}\right]\Bigg|_{\substack{s=s_{qs}\\ \eta=0}}. \tag{62}$$

If the current position of the quasisoliton s_{qs} is replaced by the arc length s, then it will uniquely specify on the plane (x,y) the trajectory $\mathbf{r}_0(s)$, along which the quasisoliton moves with the velocity $v = g(s_{qs},0)\bar{v}(g(s_{qs},0))$:

$$\frac{d\mathbf{r}_0}{ds} = \mathbf{s}_0(s), \tag{63}$$

$$\frac{d\mathbf{s}_0}{ds} = \kappa(s)\mathbf{n}_0(s) = \left[\left(1 - \frac{2\bar{\mathcal{E}}(g)}{\bar{v}(g)\bar{\mathcal{P}}(g)}\right)\frac{\partial \ln g}{\partial \eta}\right]\Bigg|_{\eta=0}\mathbf{n}_0(s), \tag{64}$$

where $\mathbf{s}_0(s)$ and $\mathbf{n}_0(s)$ are the unit vectors of the tangent and the normal to the curve $\mathbf{r}_0(s)$, respectively.

By analogy with geometrical optics, we introduce, instead of the arc length s, a new variable τ:

$$d\tau = ds/v(g(s,0)), \tag{65}$$

where the function $v(g(s,\eta))$ has the meaning of an "effective refractive index" for two-dimensional dark quasisolitons in an inhomogeneous condensate. If $v(g(s,\eta))$ is defined as

$$v(g(s,\eta)) = \beta g(s,\eta)\bar{\mathcal{P}}(g(s,\eta)), \tag{66}$$

where β is an arbitrary constant, then the equation of the quasisoliton trajectory takes the form typical of geometrical optics:

$$\frac{d\mathbf{r}_0}{d\tau} = v(g(s,0))\mathbf{s}_0 = \mathbf{p}, \tag{67}$$

$$\frac{d\mathbf{p}}{d\tau} = \frac{1}{2}\nabla\left(v^2\right)\Big|_{\eta=0}. \tag{68}$$

Using the arbitrary choice of β, we determine the effective refractive index $v(s,\eta)$ in such a way that in the low-energy limit ($\bar{\mathcal{E}} \ll 1$), where $\bar{\mathcal{P}}(s) \approx \bar{\mathcal{E}}(s) = \bar{\mathcal{E}}(0)g^2(0,0)/g^2(s,0)$, it coincides with the refractive index of sound waves, which in the dimensionless variables used is equal to $1/g(s,\eta)$. It is easy to see that this can be done by assuming

$$\beta^{-1} = \bar{\mathcal{E}}(0)g^2(0,0). \tag{69}$$

Thus, based on the analytical approach we developed, the following method can be proposed to calculate the trajectories

of two-dimensional dark quasisolitons in a smoothly inhomogeneous BEC.

(i) First of all, we seek the density distribution of the condensate formed under the action of the external potential $V_{\rm ext}(\mathbf{r})$ in the Thomas-Fermi approximation using Eq. (38). We note once again that this approximation is effective only for $[1 - V_{\rm ext}(\mathbf{r})] > 0$.

(ii) Then, using Eqs. (59) and (66), we determine the effective refractive index. Using the approximation given by Eqs. (29)–(31), we find that

$$v_{\rm TF}(\mathbf{r}) = \sqrt{n_{g_{\rm TF}}(\mathbf{r})}\,\frac{\alpha_{\rm TF}(\mathbf{r})}{\bar{\mathcal{E}}_0\, n_{0,g_{\rm TF}}}\sinh\left(\frac{\bar{\mathcal{E}}_0\, n_{0,g_{\rm TF}}}{\alpha_{\rm TF}(\mathbf{r})\, n_{g_{\rm TF}}(\mathbf{r})}\right), \tag{70}$$

$$\alpha_{\rm TF}(\mathbf{r}) = 2\pi + \frac{2\pi}{3}\exp\left[-\left(\frac{\bar{\mathcal{E}}_0\, n_{0,g_{\rm TF}}}{9.8\, n_{g_{\rm TF}}(\mathbf{r})}\right)^2\right], \tag{71}$$

where $\bar{\mathcal{E}}_0$ and $n_{0,g_{\rm TF}}$ are the normalized energy of the quasisoliton and the density of the undisturbed BEC at the point $\mathbf{r} = \mathbf{r}_0(0)$ from which the soliton starts.

(iii) Next we solve the geometrical-optics equation

$$\frac{d^2\mathbf{r}_0}{d\tau^2} = \frac{1}{2}\nabla\left(v_{\rm TF}^2\right)\Big|_{\mathbf{r}=\mathbf{r}_0} \tag{72}$$

with the "initial conditions"

$$\mathbf{r}_0(\tau = 0) = \mathbf{r}_0(t = 0), \tag{73}$$

$$\left.\frac{d\mathbf{r}_0(\tau)}{d\tau}\right|_{\tau=0} = \left[v_{\rm TF}(\mathbf{r}_0(t))\frac{\dot{\mathbf{r}}_0(t)}{|\dot{\mathbf{r}}_0(t)|}\right]\Bigg|_{t=0}. \tag{74}$$

Here, $\mathbf{r}_0(t = 0)$ and $\dot{\mathbf{r}}_0(t = 0)$ are the position and velocity of a quasisoliton at the time $t = 0$ when we started to follow its motion. Finally, we determine the trajectory $\mathbf{r}_0(\tau)$, along which a two-dimensional dark quasisoliton moves with the velocity

$$v(\mathbf{r}_0) = \sqrt{n_{g_{\rm TF}}(\mathbf{r}_0)}\;\bar{v}(\bar{\mathcal{E}}(\mathbf{r}_0)). \tag{75}$$

V. NUMERICAL SIMULATION OF THE DYNAMICS OF TWO-DIMENSIONAL DARK QUASISOLITONS IN A SMOOTHLY INHOMOGENEOUS BEC

To show the validity of the proposed method for describing the dynamics of two-dimensional dark quasisolitons in a smoothly inhomogeneous BEC, we numerically calculated the behavior of quasisolitons directly within the framework of GP equation (1) with a harmonic trap potential:

$$V_{\rm ext}(\mathbf{r}) = \frac{\omega_x^2 x^2}{2} + \frac{\omega_y^2 y^2}{2}, \tag{76}$$

where ω_x and ω_y are the dimensionless trap frequencies.

In accordance with representation (32), the wave function $\Psi(\mathbf{r},t)$ was specified at the initial time $t = 0$ in the form of the product

$$\Psi(\mathbf{r}, t = 0) = g(\mathbf{r})\, F_0(\xi,\eta,v_0). \tag{77}$$

Here, $g(\mathbf{r})$ is a purely real, positively defined, spatially localized solution of Eq. (33) with the external potential $V_{\rm ext}(\mathbf{r})$ in the form (76), $F_0(\xi,\eta,v_0)$ is the soliton solution of Eq. (45) with $v = v_0$ and $g^2(s_{\rm qs},0) = g_0^2$, $v_0 = v(t = 0) = g_0\bar{v}(\bar{\mathcal{E}}_0)$ is the initial velocity of the quasisoliton, g_0^2 is the density of the undisturbed inhomogeneous BEC at the point $\mathbf{r}_0(t = 0)$ from which the quasisoliton starts, ξ and η are the coordinates reckoned from the point $\mathbf{r}_0(t = 0)$ along and across the initial velocity vector $\mathbf{v}_0 \equiv \dot{\mathbf{r}}_0(t = 0)$ of the quasisoliton, and $\bar{\mathcal{E}}_0$ is the initial value of the normalized energy of the quasisoliton.

The parameters ω_x, ω_y, and $\bar{\mathcal{E}}_0$ were chosen such that condition (35), according to which the BEC is smooth on the scale of the localization region of a soliton-like disturbance is fulfilled. Recall that in the normalization used here, the chemical potential of the condensate is equal to unity [see Eq. (33)] and the Thomas-Fermi approximation is effective for the Bose gas density in the region where $V_{\rm ext}(\mathbf{r}) < 1$ for both $\omega_x \ll 1$ and $\omega_y \ll 1$:

$$g^2(\mathbf{r}) \approx n_{g_{\rm TF}}(\mathbf{r}) = 1 - \frac{\omega_x^2 x^2}{2} - \frac{\omega_y^2 y^2}{2}. \tag{78}$$

However, although the parameters ω_x and ω_y of the trap are small, we calculated the density distribution $g^2(\mathbf{r})$ of the undisturbed BEC without the Thomas-Fermi approximation (78), but using the numerical solution of stationary equation (33). The wave function $F_0(\xi,\eta,v_0) \equiv \Psi_s(\bar{\xi},\bar{\eta},\bar{v}(\bar{\mathcal{E}}_0))$ [see Eq. (48)] of a two-dimensional dark soliton in initial condition (77) was also found by numerical solution of stationary problem (45).

Figures 3–6 present the results of numerical simulation of GP equation (1) with initial condition (77). The cases corresponding to Figs. 3–6 differ from each other by frequencies ω_x and ω_y of harmonic trap potential (76) and by the chosen starting point $\mathbf{r}_0(t = 0)$ and normalized energy $\bar{\mathcal{E}}_0$ of a two-dimensional dark quasisoliton. In both cases, the starting velocity of the quasisoliton was directed along the x axis.

Figures 3 and 5 clearly demonstrate that two-dimensional dark quasisolitons indeed move along the trajectories shown by solid lines, which were calculated using Eq. (72). Figures 4 and 6, in turn, allow the structural changes in the quasisolitons moving along the corresponding propagation paths to be analyzed in more detail. These figures show snapshots of the density distributions [fragments (a)–(d)] and the phases of the wave function [fragments (e)–(h)] of the BEC directly in the localization region of the quasisoliton formation.

In the first case (Figs. 3 and 4), the frequencies ω_x and ω_y of harmonic potential (76) are equal to $\omega_x = 0.0135$ and $\omega_y = 0.027$. The two-dimensional dark quasisoliton starts from the point with the coordinates $x_0 = -44.82$ and $y_0 = 14.94$ and has the initial normalized energy $\bar{\mathcal{E}}_0 = 10.48$, which corresponds to the normalized velocity $\bar{v}_0 = 0.4$. Such a quasisoliton, originally given in the form of a vortex pair, remains vortical everywhere along the trajectory of motion. This is evidenced by the fact that two topological defects, or zeros of the condensate density, around which the wave function of the BEC undergoes phase jumps by $\pm 2\pi$, are present at any moment of time. It is easily seen that when the denser condensate is reached [fragments (a), (b), (e), and (f)], the vortex and antivortex forming a vortex pair approach each other, and on the contrary they diverge when moving toward the less dense condensate [fragments (c), (d), (h), and (g)].

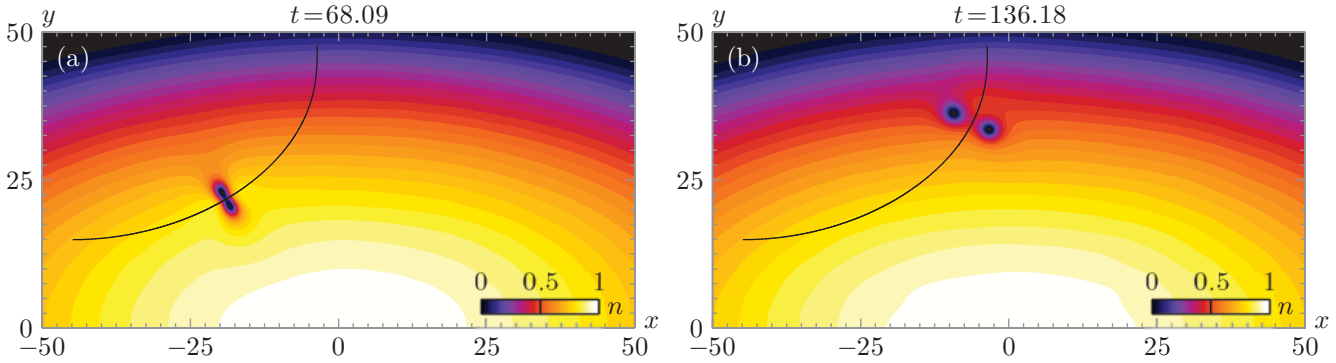

FIG. 3. (Color online) Snapshots for (a) $t = 68.09$ and (b) $t = 136.18$ of the density $n = |\Psi|^2$ of the BEC confined by a harmonic trap given by (76) with the dimensionless frequencies $\omega_x = 0.0135$ and $\omega_y = 0.027$, when a two-dimensional dark quasisoliton starting from the point with the coordinates $x_0 = -44.82$ and $y_0 = 14.94$ and having the initial normalized energy $\bar{\mathcal{E}}_0 = 10.48$ propagates. The condensate density distributions were obtained by direct numerical simulation performed directly within the framework of GP equation (1). The solid line shows the quasisoliton trajectory calculated using Eq. (72).

In the second case (Figs. 5 and 6), the trap potential (76) is specified by the frequencies $\omega_x = 0.014$ and $\omega_y = 0.028$. The vortex pair starts from the point with the coordinates $x_0 = -43.06$ and $y_0 = 7.18$ and has the normalized energy $\bar{\mathcal{E}}_0 = 8.68$, which corresponds to the normalized velocity $\bar{v} = 0.525$. With these parameters, the internal structure of the quasisoliton as it moves over an inhomogeneous BEC is substantially rebuilt. Entering the denser condensate, the vortex pair converts into a vortex-free quasisoliton, which is confirmed by the absence of the density zeros and related phase jumps of the wave function in fragments (b), (c), (f), and (g). Then, reaching the less dense BEC, the vortex-free quasisoliton again converts into a vortex pair [fragments (d) and (h)].

This behavior of two-dimensional dark quasisolitons is in full agreement with our concept that the internal structure of a quasisoliton at any time t is determined by its normalized energy $\bar{\mathcal{E}}$, whose value [see relation (59)] is inversely proportional to the density of the undisturbed inhomogeneous condensate at the center of the moving quasisoliton formation.

Variations in the normalized energy $\bar{\mathcal{E}}$ of a two-dimensional dark soliton moving along its propagation path $\mathbf{r}_0(\tau)$ in cases corresponding to Figs. 3–6 are clearly demonstrated by the diagrams A and B of the dependence $\bar{\mathcal{E}}(\tau)$ in Fig. 7. Solid lines in

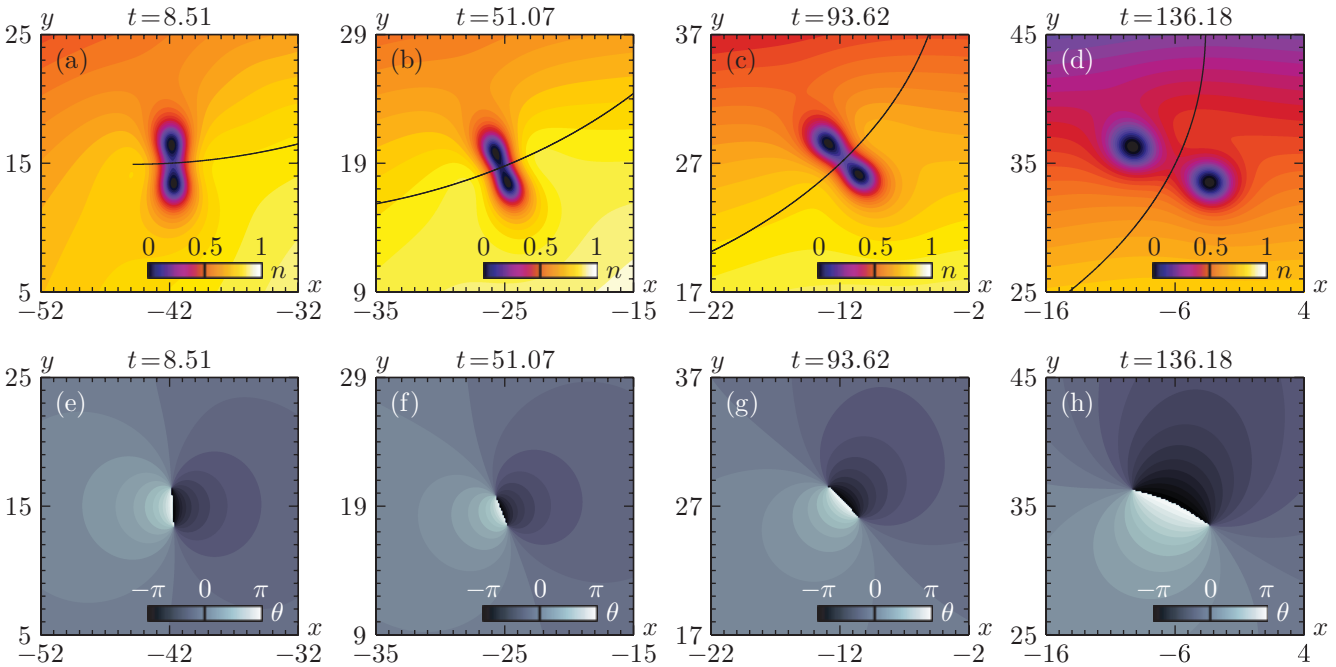

FIG. 4. (Color online) Closeups of the distributions (a)–(d) of the condensate density $n = |\Psi|^2$ and (e)–(h) of the phase $\theta = \arg(\Psi)$ of the BEC wave function at the times (a), (e) $t = 8.51$, (b), (f) $t = 51.07$, (c), (g) $t = 93.62$, and (d), (h) $t = 136.18$, which were obtained by the same numerical calculations as in Fig. 3. These distributions permit one to trace the evolution of the internal structure of a quasisoliton.

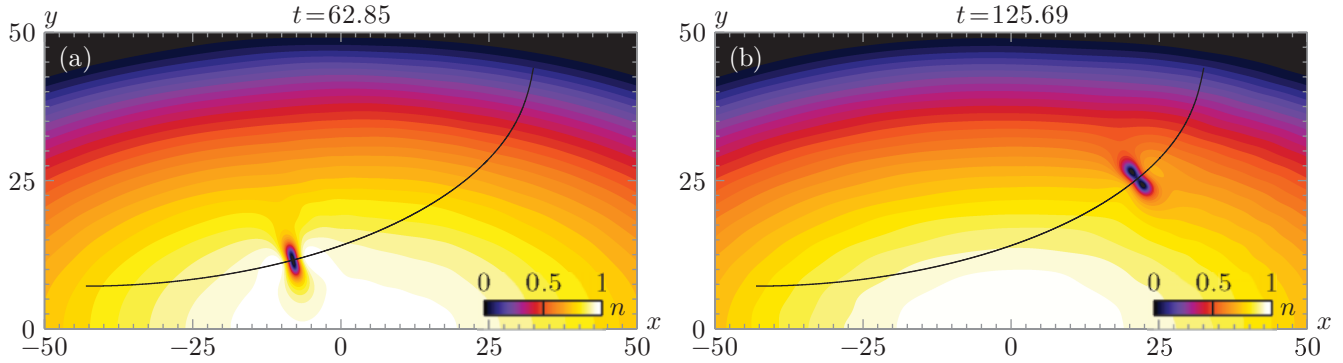

FIG. 5. (Color online) Snapshots at (a) $t = 62.85$ and (b) $t = 125.69$ of the density $n = |\Psi|^2$ of the BEC confined by a harmonic trap given by Eq. (76) with the dimensionless frequencies $\omega_x = 0.014$ and $\omega_y = 0.028$, when a two-dimensional dark quasisoliton starting from the point with the coordinates $x_0 = -43.06$ and $y_0 = 7.18$ and having the initial normalized energy $\bar{\mathcal{E}}_0 = 8.68$ propagates. The condensate density distribution were obtained by direct numerical simulation performed directly within the framework of GP equation (1). The solid line shows the quasisoliton trajectory calculated using Eq. (72).

this figure were calculated using Eq. (59). The results obtained by numerical simulation directly within the framework of GP equation (1) are marked by unshaded squares for the diagram A and unshaded circles for the diagram B. To find the normalized energy of a quasisoliton, we used the relation (14), which, as was mentioned above, permits one to determine $\bar{\mathcal{E}}$ directly from the density $n(\mathbf{r},t) = |\Psi(\mathbf{r},t)|^2$ in the localization region of the quasisoliton formation, i.e., $|\mathbf{r}|^2 < \Lambda_{qs}$.

Diagram A of the function $\bar{\mathcal{E}}(\tau)$ everywhere along the trajectory $\mathbf{r}_0(\tau)$ lies above the critical value of the annihilation $\bar{\mathcal{E}}_* \approx 7.59$. For $\bar{\mathcal{E}} = \bar{\mathcal{E}}_* \approx 7.59$, when the normalized velocity $\bar{v}$ of a quasisoliton is equal to $\bar{v}_* \approx 0.61$, the soliton state undergoes a bifurcation, and the topological defects (zeroes of the condensate density) shrink to one point (see Sec. II). Hence, the quasisoliton corresponding to Figs. 3 and 4, which is specified at the initial time $t = 0$ in the form of a vortex pair, remains vortical in the dense condensate as well.

Diagram B in a certain interval of τ is below the bifurcation value $\bar{\mathcal{E}}_* \approx 7.59$. This means that in this part of the propagation path the quasisoliton becomes vortex-free. This explains the numerical simulation results presented in Fig. 6 where zeros of the condensate density and related phase jumps by $\pm 2\pi$ of the BEC wave function disappear [see fragments (b), (c), (f), and (g)] and then appear again [see fragments (d) and (h)].

Thus, in the case of two-dimensional dark quasisolitons moving in a smoothly inhomogeneous BEC, the annihilation

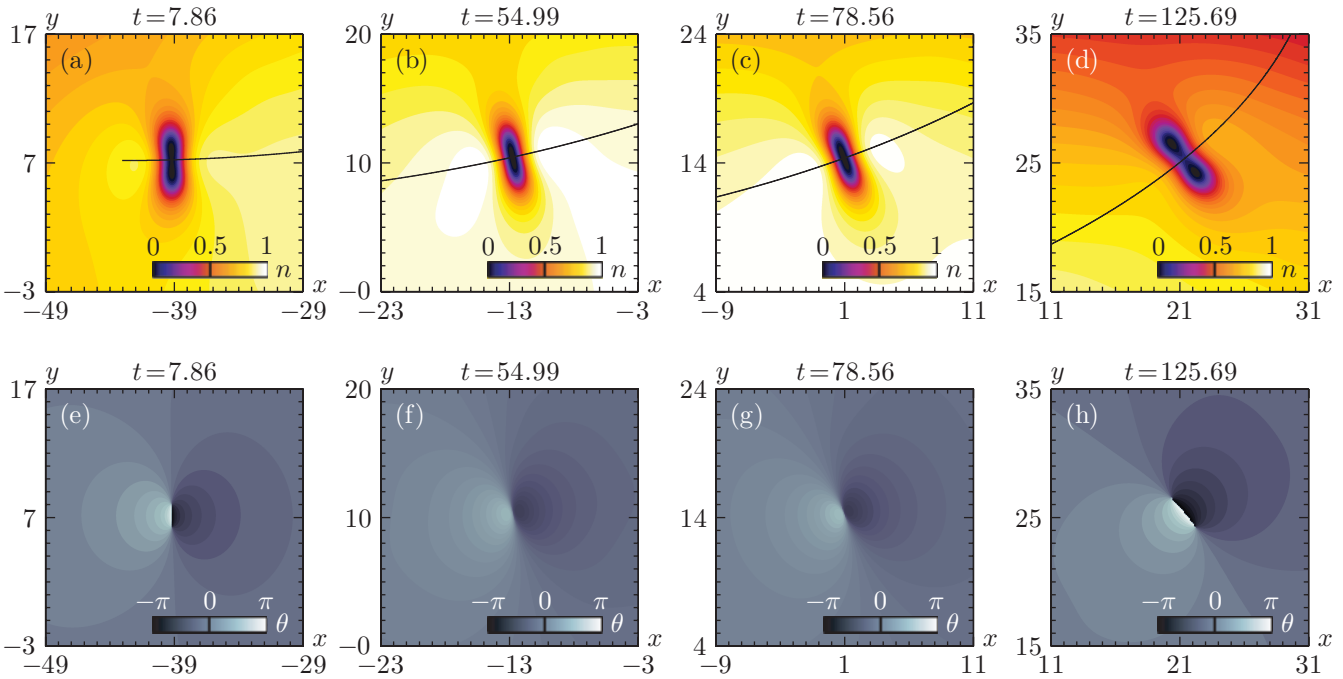

FIG. 6. (Color online) Closeups of the distributions (a)–(d) of the condensate density $n = |\Psi|^2$ and (e)–(h) of the phase $\theta = \arg(\Psi)$ of the BEC wave function at the times (a), (e) $t = 7.86$, (b), (f) $t = 54.99$, (c), (g) $t = 78.56$, and (d), (h) $t = 125.69$, which were obtained by the same numerical calculations as in Fig. 5. These distributions permit one to trace the evolution of the internal structure of a quasisoliton.

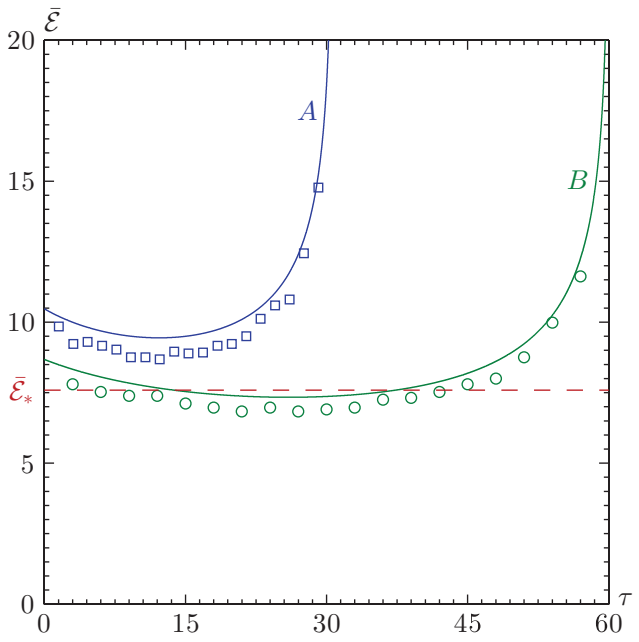

FIG. 7. (Color online) Variations in the normalized energy $\bar{\mathcal{E}}$ of a two-dimensional dark soliton along its propagation path $\mathbf{r}_0(\tau)$ in cases corresponding to the diagram *A* in Figs. 3 and 4 and to the diagram *B* in Figs. 5 and 6. The dashed line shows the critical values $\bar{\mathcal{E}} = \bar{\mathcal{E}}_* \approx 7.59$ of the normalized energy, at which the normalized velocity $\bar{v}$ of a two-dimensional dark soliton is equal to $\bar{v}_* \approx 0.61$ and the soliton state undergoes a bifurcation (the vortex two-dimensional dark soliton converts into a vortex-free one). The unshared squares and circles show the results obtained by numerical simulation performed directly within the framework of GP equation (1).

and production of vortices that form a vortex pair are a consequence of the adiabatic restructuring of the quasisoliton formation with slow variation in the density $g^2(\mathbf{r}_0)$ of the surrounding condensate. These processes are not accompanied by a tangible emission of sound waves, and the energy stored in the quasisoliton disturbance can be considered a conserved quantity [see Eq. (59)]. We note, however, that if the BEC disturbances are very different from two-dimensional quasisolitons, then the annihilation and production of vortices may lead to high radiation losses and are often "catastrophic" [58–64]. Sometimes these processes are even qualified as the collapse of vortex pairs [59–64], although unlike the two-dimensional dark solitons in the velocity range $0 < |\bar{v}| < 0.61$, they are definitely not the real stationary vortex pairs.

It follows that knowing the dependence $\bar{\mathcal{E}}(\tau)$, which is easily found from Eq. (59) after the solution of Eq. (72) for the propagation path $\mathbf{r}_0(\tau)$, one can describe the structural changes in a two-dimensional quasisoliton as it moves in a smoothly inhomogeneous BEC.

Figures 8(a) and 8(b) show the families of trajectories of two-dimensional dark quasisolitons differing in the initial normalized energy $\bar{\mathcal{E}}_0$. They start in the direction of the x axis in the same condensate as in Figs. 3–6, respectively. It is seen in Fig. 8 that quasisolitons always deflect toward the less dense condensate, and this effect increases with increasing initial normalized energy $\bar{\mathcal{E}}_0$. The shaded and unshaded circles and squares in the diagrams show the positions of the centers of the quasisolitons, which were found by numerical solution of GP equation (1).

To conclude this section, we emphasize again that the above comparisons of the results of numerical simulation of the dynamics of two-dimensional dark quasisolitons directly within GP equation (1) with the results obtained by using the asymptotic theory developed in Secs. III and IV confirm the validity of the proposed method of describing the behavior of quasisolitons in a smoothly inhomogeneous BEC.

VI. CONCLUSIONS

Thus, we have analyzed in detail the behavior of two-dimensional dark quasisolitons, namely, vortex-antivortex pairs as their particular case, in a smoothly inhomogeneous BEC at rest with repulsive interaction between atoms. The considered problem is important and very topical for the ultracold gas theory. Summarizing the work done, we briefly enlist its main results.

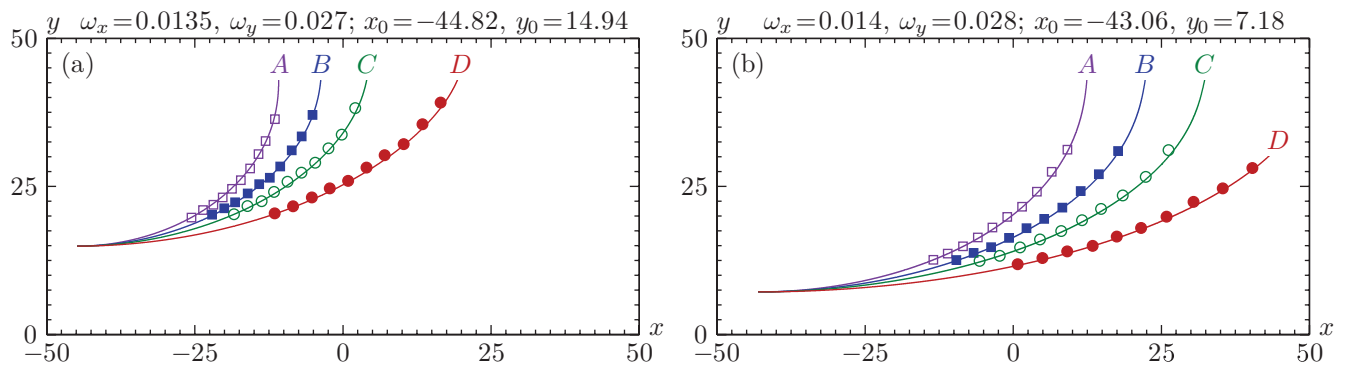

FIG. 8. (Color online) The trajectories of two-dimensional dark quasisolitons with different initial energies $\bar{\mathcal{E}}_0$: $\bar{\mathcal{E}}_0 = 12.50$ for the trajectory *A*, $\bar{\mathcal{E}}_0 = 10.48$ for the trajectory *B*, $\bar{\mathcal{E}}_0 = 8.68$ for the trajectory *C*, and $\bar{\mathcal{E}}_0 = 5.25$ for the trajectory *D*, which were calculated using Eq. (72). Quasisolitons start in the direction of the x axis from the points with coordinates (a) $x_0 = -44.82$ and $y_0 = 14.94$, (b) $x_0 = -43.06$ and $y_0 = 7.18$, and propagate, respectively, in the BEC confined in a harmonic trap (76) with dimensionless frequencies (a) $\omega_x = 0.014$ and $\omega_y = 0.028$, (b) $\omega_x = 0.014$ and $\omega_y = 0.028$. The unshared and shared squares and circles show the results obtained by numerical simulation performed directly within the framework of GP equation (1).

First, we have found the analytical approximation for the dependence of the momentum of two-dimensional dark solitons on their energy. Second, we established that the trajectories of two-dimensional dark quasisolitons in a smoothly inhomogeneous BEC are described by a system of ordinary differential equations, which we reduced to a form typical of geometrical optics of isotropic media. To this end, we introduced the concept of an effective refractive index dependent on both the density distribution of the undisturbed inhomogeneous condensate and the energy of the quasisoliton propagating in it.

Third, we have found the law of variation in the normalized energy of two-dimensional dark quasisolitons along their propagation paths. Using this law, one can describe the structural transformations of the quasisoliton formations moving in a smoothly inhomogeneous BEC. For example, as the quasisolitons reach the denser condensate, their normalized energy decreases, and the topological defects in the vortex pair begin to approach each other. Probably, they can even transform into vortex-free quasisolitons which convert into KP solitons in the limit of very high densities. In turn, vortex-free quasisolitons reaching the less dense BEC, on the contrary, convert into vortex-antivortex pairs.

Fourth, considering, as an example, the problem of the dynamics of two-dimensional dark quasisolitons originally given in the form of vortex pairs in the Bose condensate confined by a harmonic trap potential, we compared the results obtained by numerical simulation directly within the framework of the GP equation and the results of the analysis based on the constructed asymptotic description. This comparison shows good agreement between direct numerical calculations and the developed theory, which confirms its validity.

In conclusion, we note that by artificially creating inhomogeneities in the condensate, using, e.g., focused laser beams [7–9], it is possible to control the behavior of two-dimensional dark quasisolitons and, in particular, the behavior of the vortex pairs [65]. Our method of calculating the trajectories of the quasisoliton structure makes it possible to effectively select control parameters of the laser beams, which, obviously, have a very important practical application and can be used in real experiments with BEC with repulsive interaction between atoms.

ACKNOWLEDGMENTS

The authors are grateful to A. I. Smirnov for useful discussions of the results. This work was supported by the "Dynasty" Foundation.

[1] L. P. Pitaevskii and S. Stringari, *Bose-Einstein Condensation*, 2nd ed. (Clarendon, Oxford, 2003).
[2] C. Pethick and H. Smith, *Bose-Einstein Condensation in Dilute Gases*, 2nd ed. (Cambridge University Press, Cambridge, England, 2008).
[3] H. T. C. Stoof, K. B. Gubbels, and D. B. M. Dickerscheid, *Ultracold Quantum Fields* (Springer and Canopus, Bristol, 2009).
[4] P. G. Kevrekidis, D. J. Frantzeskakis, and R. Carretero-González, *Emergent Nonlinear Phenomena in Bose-Einstein Condensates: Theory and Experiment* (Springer, Berlin, Heidelberg, 2008).
[5] C. F. Barenghi, R. J. Donnelly, and W. F. E. Vinen, *Quantized Vortex Dynamics and Superfluid Turbulence* (Springer-Verlag, Berlin, Heidelberg, 2001).
[6] A. Aftalion, *Vortices in Bose-Einstein Condensates* (Birkhäuser, Boston, 2006).
[7] R. Srinivasan, Pramana - J. Phys. **66**, 3 (2006).
[8] B. P. Anderson, J. Low Temp. Phys. **161**, 574 (2010).
[9] V. A. Mironov, A. I. Smirnov, and L. A. Smirnov, JETP **110**, 877 (2010), and references therein.
[10] V. A. Mironov, A. I. Smirnov, and L. A. Smirnov, JETP **112**, 46 (2011), and references therein.
[11] P. G. Kevrekidis, R. Carretero-González, D. J. Frantzeskakis, and I. G. Kevrekidis, Mod. Phys. Lett. B **18**, 1481 (2004).
[12] A. L. Fetter and A. A. Svidzinsky, J. Phys.: Condens. Matter **13**, R135 (2001).
[13] A. L. Fetter, Rev. Mod. Phys. **81**, 647 (2009).
[14] A. L. Fetter, J. Low Temp. Phys. **161**, 445 (2010).
[15] M. Tsubota, J. Phys.: Conf. Ser. **31**, 88 (2006).
[16] B. Halperin, M. Tsubota, and W. P. E. Halperin, *Progress in Low Temperature Physics: Quantum Turbulence* (Elsevier, Amsterdam, 2008).
[17] M. Kobayashi and M. Tsubota, Phys. Rev. A **76**, 045603 (2007).
[18] M. Tsubota, J. Phys.: Condens. Matter **21**, 164207 (2009).
[19] R. Numasato, M. Tsubota, and V. S. L'vov, Phys. Rev. A **81**, 063630 (2010).
[20] N. Sasa, T. Kano, M. Machida, V. S. L'vov, O. Rudenko, and M. Tsubota, Phys. Rev. B **84**, 054525 (2011).
[21] S. Nazarenko and M. Onorato, Physica D **219**, 1 (2006).
[22] S. Nazarenko and M. Onorato, J. Low Temp. Phys. **146**, 31 (2007).
[23] D. Proment, S. Nazarenko, and M. Onorato, Phys. Rev. A **80**, 051603 (2009).
[24] A. C. White, C. F. Barenghi, N. P. Proukakis, A. J. Youd, and D. H. Wacks, Phys. Rev. Lett. **104**, 075301 (2010).
[25] T. P. Simula, Phys. Rev. A **84**, 021603 (2011).
[26] M. S. Paoletti and D. P. Lathrop, Annu. Rev. Condens. Matter Phys. **2**, 213 (2011).
[27] T. W. Neely, E. C. Samson, A. S. Bradley, M. J. Davis, and B. P. Anderson, Phys. Rev. Lett. **104**, 160401 (2010).
[28] D. V. Freilich, D. M. Bianchi, A. M. Kaufman, T. K. Langin, and D. S. Hall, Science **329**, 1182 (2010).
[29] S. Middelkamp, P. J. Torres, P. G. Kevrekidis, D. J. Frantzeskakis, R. Carretero-González, P. Schmelcher, D. V. Freilich, and D. S. Hall, Phys. Rev. A **84**, 011605 (2011).
[30] S. Middelkamp, P. G. Kevrekidis, D. J. Frantzeskakis, R. Carretero-González, and P. Schmelcher, Phys. Rev. A **82**, 013646 (2010).

[31] P. J. Torres, P. G. Kevrekidis, D. J. Frantzeskakis, R. Carretero-González, P. Schmelcher, and D. S. Hall, Phys. Lett. A **375**, 3044 (2011).

[32] P. J. Torres, R. Carretero-González, S. Middelkamp, P. Schmelcher, D. J. Frantzeskakis, and P. G. Kevrekidis, Commun. Pure Appl. Anal. **10**, 1589 (2011).

[33] J. Stockhofe, S. Middelkamp, P. G. Kevrekidis, and P. Schmelcher, Europhys. Lett. **93**, 20008 (2011).

[34] C. A. Jones and P. H. Roberts, J. Phys. A: Math. Gen. **15**, 2599 (1982).

[35] C. A. Jones, S. J. Putterman, and P. H. Roberts, J. Phys. A: Math. Gen. **19**, 2991 (1986).

[36] E. A. Kuznetsov and J. J. Rasmussen, Phys. Rev. E **51**, 4479 (1995).

[37] N. G. Berloff, J. Phys. A: Math. Gen. **37**, 1617 (2004).

[38] N. G. Berloff and P. H. Roberts, J. Phys. A: Math. Gen. **37**, 11333 (2004).

[39] S. Tsuchiya, F. Dalfovo, C. Tozzo, and L. Pitaevskii, J. Low Temp. Phys. **148**, 393 (2007).

[40] S. Tsuchiya, F. Dalfovo, and L. Pitaevskii, Phys. Rev. A **77**, 045601 (2008).

[41] G. Huang, V. A. Makarov, and M. G. Velarde, Phys. Rev. A **67**, 023604 (2003).

[42] We consider a physical situation where one degree of freedom is frozen out, and the BEC behaves as a two-dimensional (2D) system. In essence, the motion of atoms along the z axis is disregarded throughout our analysis. It is possible that when a Bose gas is confined by the harmonic potential $(m\omega_z^2 z^2/2)$ and the oscillation length $a_z = \sqrt{\hbar/m\omega_z}$ is much smaller than the healing length $a_h = \sqrt{\hbar^2/mgn_0}(a_z \ll a_h)$, where m is the atomic mass, ω_z is the axial trapping frequency, $g = 4\pi\hbar^2 a_s/m$ is the interaction coupling constant determined by the s-wave scattering length a_s ($a_s > 0$ for repulsive interactions between atoms), and n_0 is the characteristic value of the condensate density. In this cases, the energy-level spacing in the axial (z) direction greatly exceeds the interaction energy between atoms. Furthermore, we assume that the size of the undisturbed inhomogeneous BEC in the radial (xy) plane is much larger than the characteristic size of the quasisoliton excitations (with the order of the healing length a_h) considered by us. Thus, at sufficiently low temperature, the tight confinement in the z direction suppresses this degree of freedom, and the axial dependence of the BEC wave function is Gaussian, i.e., $\phi_{ho,0}(z) = (\pi a_z^2)^{-1/4}\exp(-z^2/2a_z^2)$, which corresponds to the ground harmonic oscillator state along the z axis with the zero-point oscillation energy $\mathcal{E}_{ho,0} = \hbar\omega_z/2$. The condensate dynamics becomes effectively planar and the excitations can propagate only in the x and y directions. In this limit, the BEC dynamics can be described using a two-dimensional GP equation with the two-dimensional interaction coupling constant $g_{2D} = g/(\sqrt{2\pi}a_z)$. In dimensionless GP equation (1) the coordinates $\mathbf{r} = (x,y)$ are normalized to the two-dimensional healing length $r_{c,0} = \sqrt{\hbar^2/mg_{2D}n_0}$, the time t is normalized to $t_0 = r_{c,0}/c_s$ where $c_s = \sqrt{g_{2D}n_0/m}$ is the sound velocity, the wave function $\Psi(\mathbf{r},t)$ is normalized to $\sqrt{n_0}$, and the external potential $V_{\rm ext}(\mathbf{r},t)$ is normalized to $g_{2D}n_0$.

[43] S. V. Manakov, V. E. Zakharov, L. A. Bordag, A. R. Its, and V. B. Matveev, Phys. Lett. **63**, 3 (1977).

[44] J. Satsuma and M. J. Ablowitz, J. Math. Phys. **20**, 1496 (1979).

[45] M. Ablowitz and H. Segur, *Solitons and the Inverse Scattering Transform* (Society for Industrial and Applied Mathematics, Philadelphia, 1981).

[46] M. Ablowitz and P. Clarkson, *Solitons, Nonlinear Evolution Equations and Inverse Scattering* (Cambridge University Press, Cambridge, England, 1991).

[47] Consider two independent scale transformations along the x and y axes, namely, $\Psi_s(\xi,y,\bar{v}) \to \Psi_s(a\xi,y,\bar{v})$ and $\Psi_s(\xi,y,\bar{v}) \to \Psi_s(\xi,by,\bar{v})$, where a and b are the parameters of considered scale transformations. Substituting the functions $\Psi_s(a\xi,y,\bar{v})$ and $\Psi_s(\xi,by,\bar{v})$ into variation principle (4), we arrive at the following equations: $\partial_a[\mathcal{H}(\Psi_s(a\xi,y,\bar{v})) - \bar{v}\mathcal{P}_x(\Psi_s(a\xi,y,\bar{v}))]_{a=1} = 0$ and $\partial_b[\mathcal{H}(\Psi_s(\xi,by,\bar{v})) - \bar{v}\mathcal{P}_x(\Psi_s(\xi,by,\bar{v}))]_{b=1} = 0$. These equations are fulfilled for solutions in the form of the two-dimensional dark solitons $\Psi_s(\xi,y,\bar{v})$. Then, using simple algebraic transformations, we obtain integral relations (7)–(9).

[48] J. C. Neu, Physica D **43**, 385 (1990).

[49] F. Lund, Phys. Lett. A **159**, 245 (1991).

[50] L. M. Pismen and J. Rubinstein, Physica D **47**, 353 (1991).

[51] L. M. Pismen and J. Rubinstein, Physica D **78**, 1 (1994).

[52] N. Ercolani and R. Montgometry, Phys. Lett. A **180**, 402 (1993).

[53] H. Lamb, *Hydrodynamics*, sixth ed. (Cambridge University Press, Cambridge, England, 1932).

[54] V. E. Zakharov and E. A. Kuznetsov, Physica D **18**, 455 (1986).

[55] It should be noted that the proposed consideration can, in principle, be generalized to the case where a stationary flow of BEC with $\mathbf{v}_g(\mathbf{r}) = \nabla\theta_g(\mathbf{r})$ [$\theta_g = \theta_g(\mathbf{r})$ is the nonuniform phase distribution of the wave function $G(\mathbf{r}) = g(\mathbf{r})\exp(\theta_g(\mathbf{r}))$ of the undisturbed condensate], which is smoothly varied on a characteristic scale Λ_s of a two-dimensional soliton, is present. To do this, it should be taken into account that the total velocity $v(t)\mathbf{s}_0$ of a quasisoliton [$\mathbf{s}_0$ is a unit vector of the tangent to the motion trajectory, $\mathbf{r}_0(t)$] is composed of its velocity $\mathbf{v}_s(t)$ with respect to the flow and the flow velocity $\mathbf{v}_g(\mathbf{r}_0)$ at the point $\mathbf{r} = \mathbf{r}_0(t)$, at which at the instant t the quasisoliton is located: $v(t)\mathbf{s}_0 = \mathbf{v}_s(t) + \mathbf{v}_g(\mathbf{r}_0(t))$.

[56] Y. S. Kivshar, J. Christou, V. Tikhonenko, B. Luther-Davies, and L. M. Pismen, Opt. Commun. **152**, 198 (1998).

[57] G. A. Korn and T. M. Korn, *Mathematical Handbook for Scientists and Engineers: Definitions, Theorems, and Formulas for Reference and Review* (Courier Dover, New York, 2000).

[58] M. Abraham, I. Aranson, and B. Galanti, Phys. Rev. B **52**, R7018 (1995).

[59] I. Ivonin, JETP **85**, 1233 (1997).

[60] H. Sakaguchi and T. Higashiuchi, Phys. Lett. A **359**, 647 (2006).

[61] T. Higashiuchi and H. Sakaguchi, Laser Phys. **17**, 221 (2007).

[62] A. Klein, D. Jaksch, Y. Zhang, and W. Bao, Phys. Rev. A **76**, 043602 (2007).

[63] Y. Zhang, W. Bao, and Q. Du, Eur. J. Appl. Math. **18**, 607 (2007).

[64] Y. Zhang, W. Bao, and Q. Du, SIAM J. Appl. Math. **67**, 1740 (2007).

[65] T. Aioi, T. Kadokura, T. Kishimoto, and H. Saito, Phys. Rev. X **1**, 021003 (2011).